

STACNAS: TOWARDS STABLE AND CONSISTENT DIFFERENTIABLE NEURAL ARCHITECTURE SEARCH

Li Guilin¹, Zhang Xing¹, Wang Zitong², Li Zhenguo¹, Zhang Tong³

¹Huawei Noahs Ark Lab, ²The Chinese University of Hong Kong,

³Hong Kong University of Science and Technology

{liguilin2, zhang.xing1, li.zhenguo}@huawei.com, ztwang@math.cuhk.edu.hk, tongzhang@tongzhang-ml.org

ABSTRACT

Differentiable Neural Architecture Search algorithms such as DARTS have attracted much attention due to the low search cost and competitive accuracy. However, it has been observed that DARTS can be unstable, especially when applied to new problems. One cause of the instability is the difficulty of two-level optimization. In addition, we identify two other causes: (1) Multicollinearity of correlated/similar operations leads to unpredictable change of the architecture parameters during search; (2) The optimization complexity gap between the proxy search stage and the final training leads to suboptimal architectures. Based on these findings, we propose a two-stage grouped variable pruning algorithm using one-level optimization. In the first stage, the best group is activated, and in the second stage, the best operation in the activated group is selected. Extensive experiments verify the superiority of the proposed method both for accuracy and for stability. For the DARTS search space, the proposed strategy obtains state-of-the-art accuracies on CIFAR-10, CIFAR-100 and ImageNet. Code is available at <https://github.com/susan0199/stacnas>.

1 INTRODUCTION

There are two factors that contribute to the difficulty of Neural Architecture Search (NAS problem). First, the search space is huge: the most popular *NASNet search space* (Zoph et al. (2018)) contains approximately 10^{15} models. Second, the default method to evaluate the performance of a given architecture is to fully train it from scratch, which is very time-consuming. DARTS (Liu et al. (2018)) relaxes the discrete search space to be continuous so that one can use stochastic gradient descent to simultaneously learn the architectures and model parameters on a given dataset. Unlike randomized, evolutionary, and reinforcement learning based discrete architecture search, DARTS can score every architecture in the search space by training a single architecture model, and the total computational cost is roughly the same as the training time of using the final architecture. However, the current differentiable approaches generalize poorly to new problems and variants of the search space. Several researchers have also reported that DARTS performs poorly when applied to CIFAR-100 (Zela et al. (2019); Liang et al. (2019)) and in some cases even no better than random search (Li & Talwalkar (2019)). Without understanding and remedying these problems, it will be difficult to systematically apply DARTS beyond the CIFAR-10 classification problem. The main objective of this paper is to understand the failure patterns of DARTS and propose methods to solve these problems.

We found that one cause of the instability of DARTS is due to the difficulty of two-level optimization. In addition, we identified two other causes below.

- **Multicollinearity of correlated/similar operations** such as max pooling and average pooling, as illustrated in Figure 1. When there are two operations corresponding to feature maps that are highly correlated, the architecture parameters assigned to them may no longer represent their true importance and they may also change erratically under variants of the search space;

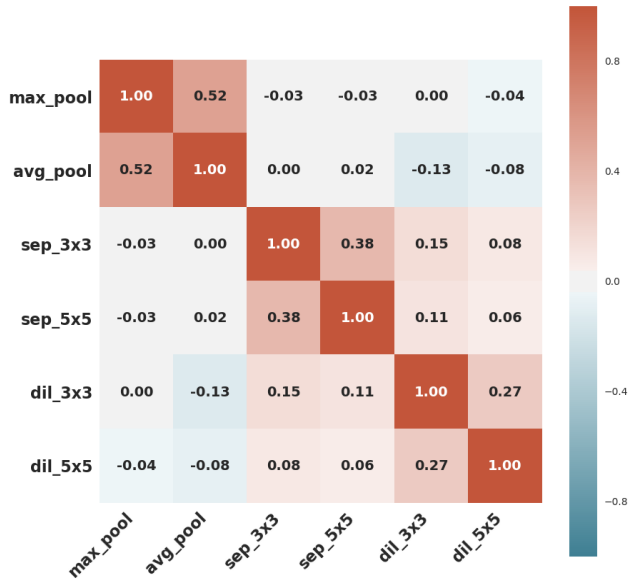


Figure 1: Grouping phenomenon of operators: correlation matrix is calculated using the flattened outputs of the six operators on the first edge of the first cell on CIFAR-10.

- The gap between the optimization complexity of the search stage architecture and the final architecture.** In our experiment with multiple datasets, when the parent architecture in the proxy search space is too shallow, the algorithms would tend to select fewer skip connections and when the parent architecture is too deep, the algorithm would select more than the optimal number of skip connections.

In this work, in addition to understanding the intrinsic problems that caused DARTS to fail, we also propose effective techniques to remedy these problems. Specially, we propose a grouped backwards pruning strategy called StacNAS (STABLE and Consistent differentiable Neural Architecture Search) based on one-level optimization. These improvements allow StacNAS to achieve the state-of-the-art performance when using the *NASNet search space* (Zoph et al. (2018)).

Our contributions on improving DARTS can be summarized as follows:

1. We propose a two-stage grouped variable pruning algorithm to compensate for the effect of multi-collinearity. This allows our method to select good operators more accurately.
2. By using **gradient confusion** (Sankararaman et al. (2019)) to measure the optimization complexity, we show that a proper depth must be selected for the proxy search architecture. We show that using this method, the system automatically selects the proper number of skip-connections for target networks with different depth (shallow or deep), while the vanilla DARTS fails to do so.
3. We show that coupled with the grouped backward variable pruning solution and optimization complexity matching, the **simpler one-level joint optimization** of both architecture and model parameters is sufficient for the *NASNet search space* with differentiable relaxation. Because it is easier to ensure convergence in one-level optimization, our method converges significantly faster, and it can scale up to complex models and large data sets, enabling direct search on ImageNet.

In our experiments in Section (3), we show that StacNAS is able to find a convolutional cell that achieves a test error of 2.33 (with same training code as DARTS for fair comparison with DARTS) and 1.78 with AutoAugmentation (Cubuk et al. (2018)) (for fair comparison with performance reported in some recent papers such as XNAS (Nayman et al. (2019))) on CIFAR-10 for image classification using around 3.6M parameters. This is the current state-of-the-art result among all NAS methods. Since we employ the simple one-level optimization, we are also able to directly search

over IMAGENET (mobile setting), and achieve a top-1 error of 24.17 (with DARTS code) and 23.22 (with additional training tricks). This result beats the current state-of-the-art *EfficientNetB0* (Tan & Le (2019)) and SCARLET-C Chu et al. (2019a) at the similar model size.

2 BACKGROUND AND RELATED WORK

2.1 SEARCH SPACE

We first use similar search space as that of DARTS, where a convolutional neural network is formed by stacking a series of building blocks called cells (Zoph et al. (2018); Real et al. (2018); Liu et al. (2018)), and only two types of cells are learned: the *normal cell* and the *reduction cell*. The only difference between them is that every reduction cell reduces the image size by a factor of 2 through the use of stride 2. Then we enlarge the search space to allow all cells in the final architecture to be different.

A cell can be seen as a directed acyclic graph (DAG) as shown in Figure 4, where an ordered sequence of N nodes $\{x_1, \dots, x_N\}$ are connected by directed edges (i, j) . Each node x_i is a latent representation (i.e. a feature map) and each directed edge (i, j) represents some operation $o(\cdot) \in O$ that transforms x_i . Within a cell, each internal node is computed as the sum of all its predecessors:

$$x_j = \sum_{i < j} o^{(i,j)}(x_i). \quad (1)$$

As in Liu et al. (2018), we include the following seven candidate operations: $\{max\ pooling\ 3 \times 3, ave\ pooling\ 3 \times 3, SepConv\ 3 \times 3, SepConv\ 5 \times 5, DilConv\ 3 \times 3, DilConv\ 5 \times 5, SkipConnect\}$. A special *zero* operation is also included to serve as a scaling factor for each edge (i, j) . According to Liu et al. (2018), for a cell with $N = 4$ nodes, this corresponds to 10^{18} possible choices of architectures.

In this framework, the task of designing the cell structure is to determine the most important two preceding edges for all internal nodes and the best choice of operations for these selected edges.

2.2 DIFFERENTIABLE RELAXATION OF NAS

DARTS (Liu et al. (2018)) proposed a continuous relaxation of the categorical choice of operations and edges so that the relative importance of them can be learned through stochastic gradient descent (SGD). Specifically, to make the search space continuous, DARTS replaces the discrete choice of operation $o(\cdot) \in O$ with a weighted sum over all candidate operations (Figure 4):

$$\bar{o}^{(i,j)}(x) = \sum_{o \in O} \alpha_o^{(i,j)} o^{(i,j)}(x_i) \quad (2)$$

where

$$\alpha_o^{(i,j)} = \frac{\exp(\beta_o^{(i,j)})}{\sum_{o' \in O} \exp(\beta_{o'}^{(i,j)})} \quad (3)$$

which is called the architecture parameters.

Intuitively, a well learned $\alpha = \{\alpha_o^{(i,j)}\}$ could represent the relative importance/contribution of the operation $o^{(i,j)}$ for transforming the feature map x_i .

After the relaxation, the task of architecture search reduces to learning a set of continuous architecture parameters $\alpha = \{\alpha^{(i,j)}\}$. Specifically, one first trains a parent/proxy network that contains all candidate operations and connections/edges through Equation 1 and Equation 3. During training, one would be able to learn which operations and which edges are redundant. After the training algorithm converges, a compact architecture is obtained by pruning the unimportant operations and edges.

In DARTS, the authors formulated the optimization of the architecture parameters α and the weights w associated with the architecture as a bi-level optimization problem (Anandalingam & Friesz (1992)), where α is treated as the upper-level variable and w as the lower-level variable:

$$\min_{\alpha} L_{val}(w^*(\alpha), \alpha) \quad (4)$$

$$\text{s.t. } w^*(\alpha) = \operatorname{argmin}_w L_{train}(w, \alpha) \quad (5)$$

where L_{train} and L_{val} represent for the training and validation loss respectively.

Evaluating Equations 5 can be prohibitive due to the expensive inner optimization. Therefore, DARTS proposed to approximate $w^*(\alpha)$ by adapting w using only a single gradient update step, and update w and α alternatively using the training and validation set respectively.

After obtaining the continuous architecture parameters α , the redundant operations and edges are pruned to obtain a compact architecture by:

1. Retaining $k = 2$ strongest predecessors for each internal node, where the importance of an edge is defined as $\max_{o \in O, o \neq zero} \alpha_o^{(i,j)}$;
2. Replacing every mixed operation with the most important operation: $\bar{o}^{(i,j)} = \operatorname{argmax}_{o \in O} \alpha_o^{(i,j)}$.

2.3 RELATED WORK

Recently, there have been many attempts to improve DARTS, including Cai et al. (2018); Xie et al. (2018); Nayman et al. (2019); Chen et al. (2019); Liang et al. (2019); Stamoulis et al. (2019). Some of them also notice the failure of two-level optimization on CIFAR100 (the algorithm would converge to a cell with all skip-connections), they impose the role of only keeping two skip-connections in the normal cell either by artificially modifying the final architecture (Chen et al. (2019)) or early stop the algorithm (Liang et al. (2019)). We believe that there should be a more automatical and generalizable solution to solve this problem.

The authors of ProxylessNAS (Cai et al. (2018)) argued that the original DARTS algorithm cannot search architectures directly on ImageNet due to its large memory footprint, and proposed to solve the memory explosion problem by sampling only one path/operation at each edge to be activated at training time of the search stage. This solution reduces the memory requirement to the same level of training the final model, and thus it is possible to directly search on large datasets such as ImageNet without using a proxy dataset. In this work, we make it possible to directly search over large dataset by the combination of one-level optimization and the design of a hierarchical (two-stage) search space, as both schemes reduce the memory requirement of our algorithm compared to the original DARTS.

Similar to ProxylessNAS Cai et al. (2018), Single-Path NAS (Stamoulis et al. (2019)) replaces the original DARTS search space by a backbone (MobileNet), where the connection graph and the operation type (identity, pooling or convolution) have been designed by the human engineers, and the problem is simplified to the selection of the kernel size of the convolution operation. They formulate the backbone search space as a simpler one-path search space and argued that for their formulation, one-level optimization was good enough. In DARTS, the authors adopted two-level optimization for the reason that when they experimenting with one-level optimization, it performs poorly than two-level and they hypothesized that one-level optimization would cause overfitting.

Although Single-Path NAS has pointed out that single-level optimization is sufficient for the simplified single-path search space, whether it can be applied to the original multi-path *NAS search space* remains open. In this work, we analyze the intrinsic reasons that cause DARTS to fail and provide solutions to remedy them.

2.4 WHEN AND WHY DARTS FAILS

2.4.1 SEVERAL FAILURE PATTERNS OF DARTS

In our extensive experiments with DARTS, we found that DARTS suffers from the following problems.

1. As shown in Figure 2, the performance variation of the architectures found by DARTS with different random initial seeds is very large. In some cases, DARTS may find architectures with worse performance than the randomly picked ones in the search space. This is also the reason why DARTS needs to use 4 GPU days to perform the search four times and then use another 1 GPU day to pick the best architecture.

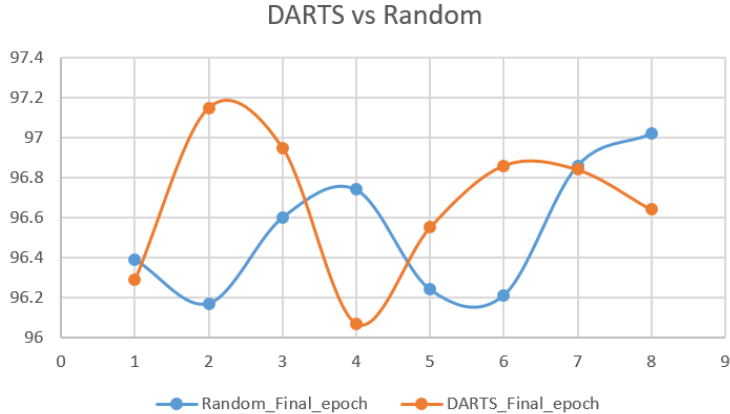


Figure 2: Repeated experiments of DARTS and randomly selected architectures

- Although DARTS works fine on CIFAR-10, it performs poorly on many other datasets. For example, on CIFAR-100, when we run DARTS until convergence, it ends up with architectures with many skip connections and poor performance. If we train the search stage for 100 epochs, all the architecture parameter of the **zero** operation would converge to 0.99.
- DARTS collapses under variants of the search space. For example, if we slightly modify the original search space as $\{max\ pooling\ 3 \times 3, SepConv\ 3 \times 3, SepConv\ 5 \times 5, SepConv\ 7 \times 7, DilConv\ 3 \times 3, DilConv\ 5 \times 5, SkipConnect, Zero\}$, the search on CIFAR10 will end up with a normal cell with dominated max pooling (Figure 3). For this case, we can only get a accuracy of 97.02 ± 0.15 on CIFAR10.
- The search results are very sensitive to the depth of the search stage architecture (i.e., the stacked number of cells). In our experiment with multiple datasets, when the search stage architecture in the proxy search space is too shallow, the algorithms would tend to select fewer skip connections and when the search stage architecture is too deep, the algorithm would select more than the optimal number of skip connections. For example, when we increase the number of cells used for the search stage from 5 to 20, the number of skip connections in the normal cell will increase from 0 to 4.

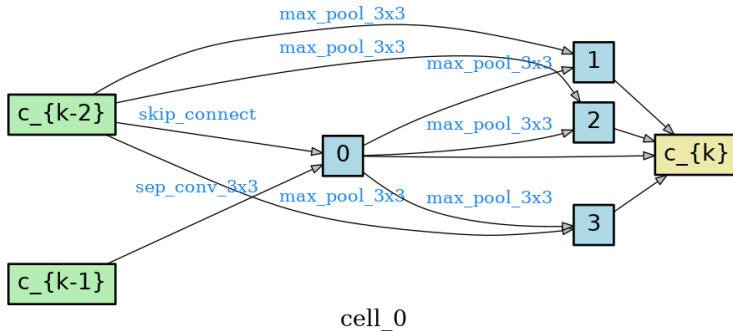


Figure 3: Normal cell dominated by max pooling found by DARTS under variants of search space

2.4.2 OUR ANALYSIS OF THE CAUSES

By analyzing these phenomena, we argue that the instability of DARTS are caused by the following three problems:

Multicollinearity of correlated operations such as max pooling and average pooling. As shown in Figure 1, there are groups of operations corresponding to feature maps that are highly correlated. For example, the correlation coefficient of max pooling and average pooling is as high as 0.52. In classical statistical literature, there is a phenomenon called multicollinearity, in which one predictor variable in a multiple regression model can be linearly predicted by other variables with a high degree of accuracy. In this situation, the architecture parameters could change erratically under the modification of the search space. Therefore, for variable selection in a multivariate regression model with collinear predictors, the values of coefficients may no longer give valid results about which predictors are redundant. Appropriate operations could be pruned as a result. This is similar to the problem caused by multicollinearity in regression.

The construction of the continuous search space as described in Section 2.1 is very similar to a multiple regression model: feature maps transformed by all candidate operations are summed together and weighted by coefficients α . The relative importance of operation o is learned through the value of α_o . When there are operations producing highly correlated feature maps (such as max pooling and average pooling), their weights α may no longer be representative of their real importance. To measure the operation correlation, we adopt the same procedure as Gastaldi (2017): we calculated the correlation between the flattened feature map of two operations for the first edge of the first cell, the results are presented in Figure 1. The details of the correlation calculation procedure are provided in the Appendix B.

To verify the conjectures about multicollinearity would cause the system to prune important operations, we conducted an experiment with CIFAR-10, including an unbalanced number of operations from different groups in the search space, such as

$$\{maxpooling3 \times 3, SepConv3 \times 3, SepConv5 \times 5, Zero\} \tag{6}$$

This ends up with a normal cell dominated with max pooling, although the architecture would have higher validation accuracy if separable convolutions are selected. The cause of this problem is due to the multicollinearity of the two separable convolutions so that they produce feature maps linearly correlated, which splits the contribution in the mixed operation. In the extreme condition, suppose they produce exactly the same feature maps, there is only one degree of freedom for them as long as

$$\alpha_{sep3 \times 3} + \alpha_{sep5 \times 5} = \alpha_{sep} \tag{7}$$

The optimization complexity gap between the proxy search stage and the final training lead to improper amount of skip connection selected. As well studied (He et al. (2016); Sankararaman et al. (2019)), including skip connections would make the gradient flows easier and optimization of the deep neural network more stable. Therefore, an ideal NAS algorithm should be able to automatically select the proper amount of skip connections desired for different network depth, i.e., select more skip-connection for deep networks to allow the gradient to flow easier and optimization of the deep network perform better. In DARTS, to save memory print, a shallow network with 8 cells are used for the search stage and a deep network with 20 cells are used for the final architecture. This depth gap causes a huge optimization complexity gap between them, and the system would not be able to foresee the optimization difficulty when the cells are stacked to a much deeper network. An improper number of skip-connections may be selected as a result.

The difficulty of bi-level optimization: the optimization algorithm relies on approximating the optimal w^* with a one-step updated w_t with a second-order approximation, which is slow and poorly regularized. The original training data has to be split into training data and validation data. With the current 1:1 split ratio, only half of the data could be used to learn w . The learning of model parameter w can be negatively affected due to the lack of data. For example, on CIFAR-100, which contains more classes with fewer images in each class than CIFAR-10, the original DARTS algorithm selects cells dominated with skip connection and a large scaling α_{zero} .

2.5 OUR SOLUTIONS

2.5.1 GROUPED VARIABLE PRUNING

To remedy this problem, we propose a two-stage grouped backward variable pruning strategy for selecting the best operations as shown in Figure 4 and Algorithm 1.

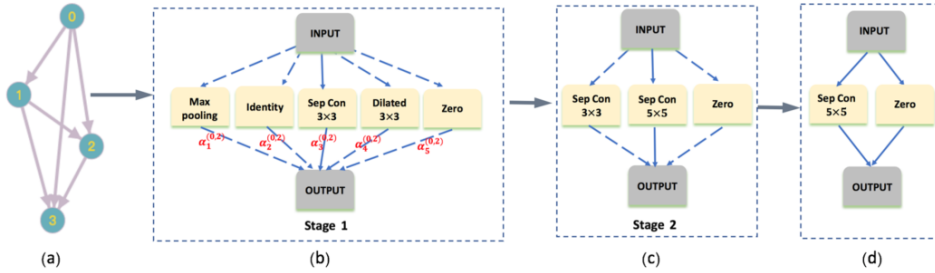


Figure 4: An overview of StacNAS: (a) A cell is a DAG with nodes connected by unknown operations. (b) Improved continuous relaxation by placing a by-group mixture of candidate operations on each edge. (c) When a certain type of operation is activated, include all candidate operations in this type to form a new mixture operation. (d) Deriving the final architecture.

The correlation matrix presented in Figure 1 suggests that max pooling and average pooling are in one group (their correlation is 0.52), 3×3 and 5×5 *SepConv* are in the same group (correlation 0.38), 3×3 and 5×5 *DilConv* are in the same group (correlation 0.27). Therefore, there should be four groups in the original DARTS search space:

- Group 1: *SkipConnect*
- Group 2: *Max pooling* 3×3 , *Ave pooling* 3×3 ;
- Group 3: *SepConv* 3×3 , *SepConv* 5×5 ;
- Group 4: *DilConv* 3×3 , *DilConv* 5×5 ;

At stage 1, we only include one operation from each group to prevent the multicollinearity phenomenon. For example, we let the following four operations serve as representatives of each group to compete first to decide which types of operation to use at edge (i, j) :

$$\{ \text{Max pooling } 3 \times 3, \text{ SkipConnect}, \text{ SepConv } 3 \times 3, \text{ DilConv } 3 \times 3 \}$$

At stage 2, suppose that the operator *SepConv* 3×3 is selected at edge (i, j) , we then replace the mixed operation $\hat{\delta}^{(i,j)}$ with a weighted sum of all operations in the same group (Group 3). Again, at every stage, a special *zero* operation is also included to serve as a scaling factor for each edge (i, j) .

Variants of search space: Note that suppose the proposed algorithm is used for variants of search space different from that of DARTS, we need to first estimate the correlation matrix of all the candidate operators to identify the underlying groups for the given data (the estimation procedure is provided in the Appendix Section B). and then select the representative operators for each group to obtain the search space of search stage 1. Although our experiments show that the final performance is not sensitive to different selections of representatives for the first stage, we would prefer to let the operations with same/similar kernel size to compete with each other.

2.5.2 OPTIMIZATION COMPLEXITY MATCHING

In our experiment with multiple datasets, when the search stage architecture is too shallow, the algorithms would tend to select fewer skip connections and when the search stage architecture is too deep, the algorithm would select more than the optimal number of skip connections. Both these two scenarios lead to poor performance of the final architecture.

In DARTS, a stack of 8 cells are used to serve as the proxy parent network during the search stage (due to the high memory cost of bi-level optimization), and then a stack of 20 cells are used to build the final architecture. This introduces a significant gap between the optimization complexity of the proxy search architecture and the final architecture.

As well studied (He et al. (2016); Sankararaman et al. (2019)), including skip connections would make the gradient flows easier and optimization of the deep neural network more stable. Therefore, whether a NAS algorithm can select the proper amount of skip connections and their location would significantly affect the performance of the designed architecture. Hence, properly matching the

Algorithm 1 Stable and Consistent Differentiable NAS

- 1: **procedure** STAGE 1 (Group search)
 - 2: Create a by-group operation $\tilde{o}^{(i,j)}(x)$ parametrized by $\tilde{\alpha}_o^{(i,j)}$ for each edge (i, j)
 - 3: **if** $t < T$ **then**
 - 4: Update weights w_t by descending $\partial_w L_{train}(w_{t-1}, \tilde{\alpha}_{t-1})$
 - 5: Update architecture parameter $\tilde{\alpha}_t$ by descending $\partial_{\tilde{\alpha}} L_{train}(w_{t-1}, \tilde{\alpha}_{t-1})$
 - 6: Set optimal $\tilde{\alpha}^* = \alpha^T$
 - 7: Activate the optimal operation group based on $\tilde{\alpha}^*$
 - 8: **procedure** STAGE 2 (Backward)
 - 9: Use all the group member of $o^{*(i,j)}$ to create mixed operation $\hat{o}^{(i,j)}(x)$ parametrized by $\hat{\alpha}_o^{(i,j)}$
 - 10: **if** $t < T$ **then**
 - 11: Update weights w_t by descending $\partial_w L_{train}(w_{t-1}, \hat{\alpha}_{t-1})$
 - 12: Update architecture parameter α_t by descending $\partial_{\alpha} L_{train}(w_{t-1}, \hat{\alpha}_{t-1})$
 - 13: Set optimal $\hat{\alpha}^* = \alpha^T$
 - 14: Select the best operation $o^{*(i,j)} \leftarrow \operatorname{argmax}_{o \in O} \hat{\alpha}^{(i,j)}$
 - 15: **procedure** STAGE 3 (Final Architecture)
 - 16: Prune the redundant operations and edges.
-

search stage and final stage optimization complexity is vital towards a consistent optimization of the system.

To quantify the optimization difficulty more concretely, we use a measurement called gradient confusion, introduced in (Sankararaman et al. (2019)). The authors empirically show that when gradient confusion is high, stochastic gradients produced by different mini-batches may be negatively correlated, slowing down convergence. But when gradient confusion is low, SGD has better convergence properties. Deeper networks usually correspond to higher gradient confusion, and skip connection can significantly reduce gradient confusion.

Formally, gradient confusion is defined to be an upper bound of the negative inner product between gradients evaluated at all mini-batches. Formally, let $\{L_i\}_{i=1}^m$ be losses for mini-batches, and let W be trainable parameters. Then a gradient confusion $\zeta \geq 0$ at W could be estimated by the following formula

$$\zeta = \max\{0, \max_{i,j=1,\dots,m} \{- \langle \nabla L_i(W), \nabla L_j(W) \rangle\}\}$$

In Table 1, we present the estimated gradient confusion for both search stage and final architecture with different depth (details are provided in the Appendix D), we can see that the desired depth (number of cells stacked) for the two search stages are 14 cells and 20 cells correspondingly, to make their optimization complexity compatible with that of the final architecture. This matching allows the proposed algorithm to be able to optimize the search architecture with the same level of difficulty with the final architecture. We find that by matching the optimization complexity, the system would automatically select the optimal number of skip connections.

Architecture depth	gradient confusion
Final Arch_20cells	0.57
Search_stage1_14cell	0.56
Search_stage1_17cell	0.87
Search_stage1_20cell	1.02
Search_stage2_20cell	0.52

Table 1: Gradient Confusion Estimation

2.5.3 ONE-LEVEL OPTIMIZATION

The author of DARTS advocate that one-level optimization would cause overfitting problem, and hereby two-level is adopted. We also conducted the one-level optimization experiment with 8 cells

for search stage, the search ends up with a normal cell with all *SepConv* 3×3 and no *SkipConnet*, which is inferior to those with, for example, two *SkipConnet* operators.

However, increase the number of cells from 8 to 20, the algorithm can find cells with increasing *SkipConnet* operators. Therefore, we advocate that the overfitting phenomenon is not caused by one-level optimization, it is caused by the optimization complexity gap as mentioned in the previous Sections.

In our ablation study in Section 3.4, we show that coupled with the solutions proposed in Section 2.5.1 and Section 2.5.2, one-level optimization performs superior to two-level optimization with respect to both accuracy and stableness. Therefore, in this work, we advocate that the architecture parameter α and architecture weights w should be optimized simultaneously using one-level optimization. We show that the proposed StacNAS based on one-level optimization can achieve the state-of-the-art performance.

Formally, in this work, we employ one-level optimization, where we jointly optimize both the architecture parameter α and the model parameter w . In our experiment, we use all of the original training data to update α and w together by descending on w and α using

$$w_t = w_{t-1} - \eta_t \partial_w L_{train}(w_{t-1}, \alpha_{t-1}) \tag{8}$$

$$\alpha_t = \alpha_{t-1} - \delta_t \partial_\alpha L_{train}(w_{t-1}, \alpha_{t-1}) \tag{9}$$

simultaneously, where η_t and δ_t are learning rates.

3 EXPERIMENTS

In this section, we validate the effectiveness of our proposed method for the image classification task.

3.1 NOTES ON FAIR EVALUATION OF NAS METHODS

In the current NAS solutions, the reported accuracies come from three sources: the search space; the search method; and the final tricks such as data augmentation to train the model. To fairly investigate the contribution of our proposed search method, in our StacNAS(base) experiments, we control both the search space and the training tricks exactly the same with DARTS. Therefore, we can conclude that the performance improvement of the whole process is truly from the proposed search method.

For reprehensibility, we reported the mean and standard deviation over 8 single runs (i.e. search once and evaluate once, repeats the procedure 8 times with different seeds). Note that for many other NAS methods like DARTS, 4 searches are conducted to pick the best one, but all our results are random ones without the selection procedure.

For fair comparison with other recent works adopting AutoAugmentation and additional tricks such as Nayman et al. (2019), the results with AutoAugmentation (Cubuk et al. (2018)) are also reported as StacNAS(AA).

3.2 NAS BENCHMARKS ON CIFAR10/CIFAR100

Datasets: We conduct our first set of experiments on CIFAR-10 and CIFAR-100 (Krizhevsky et al. (2009)), each containing 50,000 training RGB images and 10,000 test images.

Implementation Details: In the first stage, the proxy parent network of 14 cells is trained using one-level optimization for 80 epochs. After convergence, the optimal operation group is activated based on the learned α . In the second stage, we replace the mixed operation $\hat{o}^{(i,j)}$ with a weighted sum of all operations in the activated group from stage 1. Then a proxy parent network by stacking 20 cells is trained using one-level optimization for 80 epochs. Other training details are provided in the Appendix C

All of our experiments for CIFAR10 and CIFAR100 were performed using NVIDIA Tesla V100 GPUs.

Search Results: The search results are provided in Table 3 and 4. The plot of the found cells are provided in the Appendix Section E.

We can see that either by controlling the search space and training methods, or using extra training tricks, our approach achieves state-of-the-art performance on both CIFAR10 and CIFAR100.

Table 2: ImageNet Benchmark (mobile setting). **C10/C100 (base)** represents that the architectures are searched over CIFAR10/CIFAR100 and transferred to IMAGENET with the final architecture trained the same as DARTS. **IMAGENET(base)** represents that the architecture are directly searched over IMAGENET and trained the same as DARTS. **(AA)** represents that the architecture are trained with additional regularization (see Appendix C)

Architecture	Test Error (%)		Params (M)	GPU Days	Search Method
	top-1	top-5			
AmoebaNet-C Real et al. (2018)	24.3	7.6	6.4	3150	evolution
DARTS Liu et al. (2018)	26.7	8.7	4.7	4	SGD
ProxylessNAS Cai et al. (2018)	24.9	N/A	N/A	8.3	SGD
SNAS Xie et al. (2018)	27.3	9.2	4.3	1.5	SGD
PDARTS Chen et al. (2019)	24.4	7.4	4.9	0.3	SGD
PC-DARTS (ImageNet) Xu et al. (2019)	24.2	7.3	5.3	3.8	SGD
EfficientNet-B0 Tan & Le (2019)	23.7	6.8	5.3	N/A	RL
Single-Path NAS Stamoulis et al. (2019)	25.04	7.79	4.3	0.15	SGD
FairNAS-A Chu et al. (2019b)	24.66	7.62	4.6	12	SGD
SCARLET-A Chu et al. (2019a)	23.1	6.6	6.7	12	Evolution
SCARLET-C Chu et al. (2019a)	24.4	7.4	6.0	12	Evolution
StacNAS C10 (base)	24.4	7.3	5.3	1	SGD
StacNAS C10 (AA)	23.48	6.4	5.3	1	SGD
StacNAS C100 (base)	24.34	7.1	4.9	1	SGD
StacNAS (IMAGENET)(base)	24.17	6.9	5.7	20	SGD
StacNAS (IMAGENET)(AA)	23.22	5.9	5.7	20	SGD

3.3 NAS BENCHMARKS ON IMAGENET

Thanks to the simplicity of one-level optimization, we could directly search over IMAGENET without subsampling. We use 11 cells for the first search stage and 14 cells for the second search stage. And the batch size for search is 1,024. The searched normal and reduction cells are provided in Appendix Section E. We use Tesla 8*V100 GPUs for all experiments with IMAGENET. Results are summarized in Table 2. We achieve a top-1/5 accuracy of 23.22%/5.9%, which is the best known performance to date with less than 6M parameters.

Other training details are provided in Appendix C.

Table 3: CIFAR-10 Benchmark. *base* represents for that the final architecture training procedure is exactly the same with DARTS for a fair comparison; *AA* represents for that the final training adopts additional training tricks such as AutoAugmentation for comparison with other NAS methods.

Architecture	Test Error (%)		Params (M)	GPU days
	Best	Average		
DARTS (base) Liu et al. (2018)	-	2.76±0.09	3.3	4
Proxyless (AA) Cai et al. (2018)	2.08	-	5.7	4
SNAS (base) Xie et al. (2018)	-	2.85 ±0.02	2.9	1.5
PDARTS (base) Chen et al. (2019)	2.5	-	3.4	0.3
PC-DARTS(base) Xu et al. (2019)	-	2.57 ±0.07	3.6	0.1
DARTS+ (AA) Liang et al. (2019)	2.20	2.37 ± 0.13	4.3	0.6
XNAS-S (AA) Nayman et al. (2019)	1.81	-	3.7	0.3
StacNAS(base)	2.33	2.48±0.08	3.9	0.8
StacNAS(AA)	1.77	2.02 ±0.06	3.9	0.8

Table 4: CIFAR-100 Benchmark: * The results of DARTS are performed by us using the publicly available code

Architecture	Test Error (%)		Params (M)	GPU days
	Best	Average		
DARTS*(base) Liu et al. (2018)	N/A	17.54 ± 0.27	3.8	1
PDARTS (base) Chen et al. (2019)	15.92	N/A	3.6	0.3
DARTS+(AA) Liang et al. (2019)	14.87	15.45 ± 0.30	3.9	0.5
StacNAS(Base)	15.90	16.11 ± 0.2	4.3	0.8
StacNAS(AA)	13.6	14.3 ± 0.18	4	0.8

3.4 ABLATION EXPERIMENTS

Contribution of each component: In this part, we conduct experiments to check how much each of the proposed components including one-level optimization, two-stage group backwards, complexity matching, contributes to the final performance. As we can see from Table 5, both one-level and two-level optimization could benefit by the two-stage strategy and complexity match. But one-level optimization is superior to two-level.

Table 5: Ablation Experiments

	CIFAR10	
	two-level	one-level
baseline	2.97 ± 0.32	2.74 ± 0.12
grouped backward (GB)	2.82 ± 0.26	2.68 ± 0.10
GB+complexity match	2.73 ± 0.23	2.48 ± 0.08

Variants of search space: when we slightly modify the search space by replacing the original *ave pooling* 3×3 by *SepConv* 7×7 , the original DARTS ends up with normal cells dominated with *max pooling* (see Figure 3), and a validation error 2.98 ± 0.15 on CIFAR10. On the contrary, the proposed StacNAS performs robustly under this change, achieving a validation accuracy of 2.55 ± 0.08 on CIFAR10.

Stacking layers: The validation error on CIFAR10 of 8 repeated experiments for 8cells+8cells is 2.74 ± 0.12 , for 14cells+17cells is 2.58 ± 0.07 , for 17cells+20cells is 2.53 ± 0.05 , which are all inferior to the result of 14cells+20cells.

Selection of representative operations: We also experiment on CIFAR10 with randomly selected operations from each group for stage 1. The results for CIFAR10 are 2.53 ± 0.08 , which means the selection of the operations for the first stage is not sensitive. **Predicted Performance Correlation (CIFAR-10)** In differentiable NAS, the learned architecture parameter α is supposed to represent the relative importance of one candidate operation verse the others. To check the correlation between the accuracy of a stand-alone architecture with different candidate operations and the corresponding α , we replace the selected operation in the first edge of the first cell for the final architecture with all the other candidate operations in the first stage of StacNAS, and fully train them until converge. The obtained stand-alone accuracy is compared with the corresponding α learned for each candidate operation. Their correlation is plotted in Figure 5.

4 CONCLUSION

This paper introduced a stable and consistent optimization solution to differentiable NAS, which we call StacNAS. Our method addresses some difficulties encountered in the original DARTS algorithm such as bi-level optimization, multicollinearity of correlated operations, and the fundamental challenges of matching neural network optimization complexity in NAS and in the final training. It was shown that our method leads to the state-of-the-art image classification results on multiple benchmark datasets.

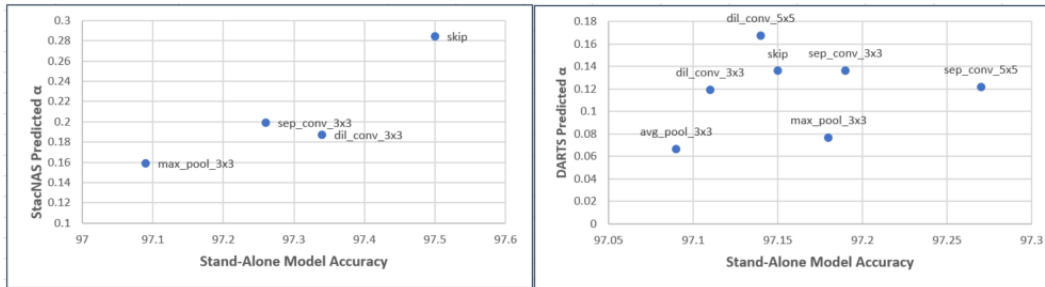


Figure 5: Correlation between standalone model and learned α : (a) Correlation coefficient of StacNAS: 0.91; (b) Correlation coefficient of DARTS: 0.2.

REFERENCES

- G Anandalingam and Terry L Friesz. Hierarchical optimization: An introduction. *Annals of Operations Research*, 34(1):1–11, 1992.
- Han Cai, Ligeng Zhu, and Song Han. Proxylessnas: Direct neural architecture search on target task and hardware. *arXiv preprint arXiv:1812.00332*, 2018.
- Xin Chen, Lingxi Xie, Jun Wu, and Qi Tian. Progressive differentiable architecture search: Bridging the depth gap between search and evaluation. *arXiv preprint arXiv:1904.12760*, 2019.
- Xiangxiang Chu, Bo Zhang, Jixiang Li, Qingyuan Li, and Ruijun Xu. Scarletnas: Bridging the gap between scalability and fairness in neural architecture search. *arXiv preprint arXiv:1908.06022*, 2019a.
- Xiangxiang Chu, Bo Zhang, Ruijun Xu, and Jixiang Li. Fairnas: Rethinking evaluation fairness of weight sharing neural architecture search. *arXiv preprint arXiv:1907.01845*, 2019b.
- Ekin D Cubuk, Barret Zoph, Dandelion Mane, Vijay Vasudevan, and Quoc V Le. Autoaugment: Learning augmentation policies from data. *arXiv preprint arXiv:1805.09501*, 2018.
- Xavier Gastaldi. Shake-shake regularization. *arXiv preprint arXiv:1705.07485*, 2017.
- Kaiming He, Xiangyu Zhang, Shaoqing Ren, and Jian Sun. Identity mappings in deep residual networks. In *European conference on computer vision*, pp. 630–645. Springer, 2016.
- Alex Krizhevsky, Vinod Nair, and Geoffrey Hinton. Cifar-10 and cifar-100 datasets. *URL: https://www.cs.toronto.edu/kriz/cifar.html*, 6, 2009.
- Liam Li and Ameet Talwalkar. Random search and reproducibility for neural architecture search. *arXiv preprint arXiv:1902.07638*, 2019.
- Hanwen Liang, Shifeng Zhang, Jiacheng Sun, Xingqiu He, Weiran Huang, Kechen Zhuang, and Zhenguo Li. Darts+: Improved differentiable architecture search with early stopping. *arXiv preprint arXiv:1909.06035*, 2019.
- Hanxiao Liu, Karen Simonyan, and Yiming Yang. Darts: Differentiable architecture search. *arXiv preprint arXiv:1806.09055*, 2018.
- Niv Nayman, Asaf Noy, Tal Ridnik, Itamar Friedman, Rong Jin, and Lihi Zelnik-Manor. Xnas: Neural architecture search with expert advice. *arXiv preprint arXiv:1906.08031*, 2019.
- Esteban Real, Alok Aggarwal, Yanping Huang, and Quoc V Le. Regularized evolution for image classifier architecture search. *arXiv preprint arXiv:1802.01548*, 2018.
- Karthik A Sankararaman, Soham De, Zheng Xu, W Ronny Huang, and Tom Goldstein. The impact of neural network overparameterization on gradient confusion and stochastic gradient descent. *arXiv preprint arXiv:1904.06963*, 2019.

- Dimitrios Stamoulis, Ruizhou Ding, Di Wang, Dimitrios Lymberopoulos, Bodhi Priyantha, Jie Liu, and Diana Marculescu. Single-path nas: Designing hardware-efficient convnets in less than 4 hours. *arXiv preprint arXiv:1904.02877*, 2019.
- Mingxing Tan and Quoc V Le. Efficientnet: Rethinking model scaling for convolutional neural networks. *arXiv preprint arXiv:1905.11946*, 2019.
- Sirui Xie, Hehui Zheng, Chunxiao Liu, and Liang Lin. Snas: stochastic neural architecture search. *arXiv preprint arXiv:1812.09926*, 2018.
- Yuhui Xu, Lingxi Xie, Xiaopeng Zhang, Xin Chen, Guo-Jun Qi, Qi Tian, and Hongkai Xiong. Pc-darts: Partial channel connections for memory-efficient differentiable architecture search. *arXiv preprint arXiv:1907.05737*, 2019.
- Arber Zela, Thomas Elsken, Tonmoy Saikia, Yassine Marrakchi, Thomas Brox, and Frank Hutter. Understanding and robustifying differentiable architecture search. *arXiv preprint arXiv:1909.09656*, 2019.
- Barret Zoph, Vijay Vasudevan, Jonathon Shlens, and Quoc V Le. Learning transferable architectures for scalable image recognition. In *Proceedings of the IEEE conference on computer vision and pattern recognition*, pp. 8697–8710, 2018.

	avg_3x3	max_3x3	sep_3x3	sep_5x5	dil_3x3	dil_5x5
avg_pool_3x3	1.00	0.52	-0.03	-0.03	0.00	-0.04
max_pool_3x3	0.52	1.00	0.00	0.02	-0.13	-0.08
sep_conv_3x3	-0.03	0.00	1.00	0.38	0.15	0.08
sep_conv_5x5	-0.03	0.02	0.38	1.00	0.11	0.06
dil_conv_3x3	0.00	-0.13	0.15	0.11	1.00	0.27
dil_conv_5x5	-0.04	-0.08	0.08	0.06	0.27	1.00

Table 6: Operator Correlation Matrix

A APPENDIX

B OPERATOR CORRELATION ESTIMATION

We Compute the correlations among different operators using CIFAR-10. This is for the purpose of grouping similar operators in our procedure. The correlation measures are obtained as follows.

1. A network of 14 cells is trained 100 epochs using parameters in the original DARTS, where the cell DAG consists four intermediate nodes and fourteen learnable edges, and each edge is a weighted summation of all the eight operators in the space.
2. With the trained model, for a given training image, we may pass it through the network, and store the output of the six operators (exclude "none" and "skip_connect") on all edges. On each edge, flatten the six output tensors into six vectors. Repeat until more than 10000 images in the training set have been processed.
3. Use the resulting data to calculate the correlations among the operators.

The resulting correlation matrix for the operators are presented in Table 6. The table clearly shows three distinct pairs of highly correlated operators, which form the three groups (plus a separate group for the skip_connect operator) in our method.

C TRAIN DETAILS

CIFAR-10 and CIFAR-100 The final architecture is a stack of 20 cells: 18 normal cells and 2 reduction cells, positioned at the 1/3 and 2/3 of the network respectively. For the *base* training, we trained the network exactly the same with DARTS. For the *fancy* training, we add AutoAugment (CIFAR10) (Cubuk et al. (2018)) policy and trained the network for 1200 epochs, other than these, all the other settings are same as DARTS.

ImageNet The final architecture is a stack of 14 cells: 12 normal cells and 2 reduction cells, positioned at the 1/3 and 2/3 of the network respectively. For the *base* training, we trained the network exactly the same with DARTS. For the *fancy* training, we add AutoAugment (IMAGENET) (Cubuk et al. (2018)) policy and SE (hu2018squeeze), then trained the network for 800 epochs, other than these, all the other settings are same as DARTS.

D ESIMATION OF GRADIENT CONFUSION

We compared gradient confusion for several different settings, including different numbers of cells, different stages, with/without an auxiliary head. The result are provided in the following table.

For each setting, we first train the architecture for 100 epochs and then ran 10 more iterations with randomly selected mini-batch using the trained parameters and compute the gradient confusion using formula (2.5.2) and obtain ζ_i for each iteration i . Then, we compute the mean of the 10 ζ_i we got and divided them by the corresponding model parameter size M . Formally,

$$\bar{\zeta} = \sum_{i=1}^{10} \zeta_i / M \tag{10}$$

We treat it as the measurement of the optimization complexity for the corresponding setting.

E CELLS OF BENCHMARK DATASET

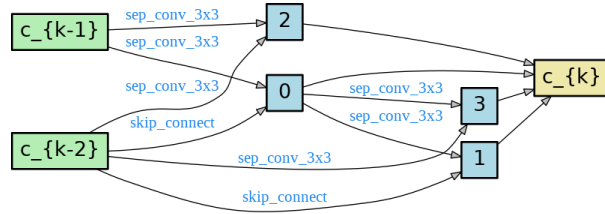


Figure 6: Normal cell learned on CIFAR-10

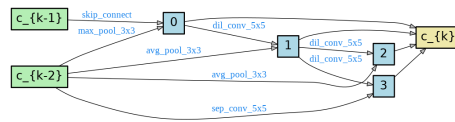


Figure 7: Reduction cell learned on CIFAR-10

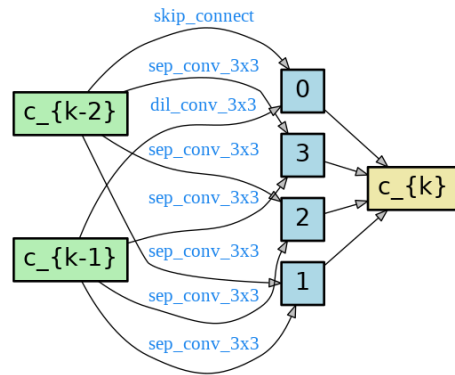


Figure 8: Normal cell learned on CIFAR-100

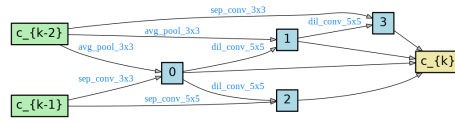


Figure 9: Reduction cell learned on CIFAR-100

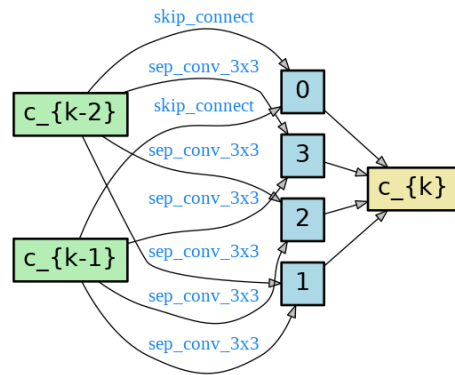


Figure 10: Normal cell learned on IMAGENET(mobile setting)

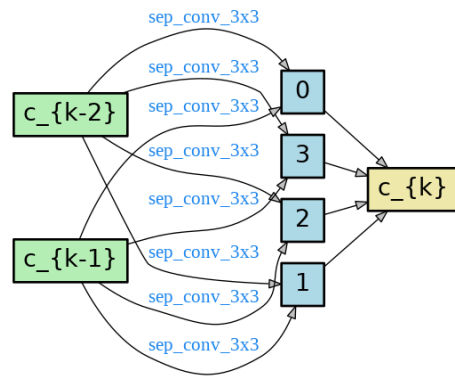


Figure 11: Reduction cell learned on IMAGENET(mobile setting)